Increased Epicardial Adipose Tissue Volume Correlates With Cardiac Sympathetic Denervation in Patients With Heart Failure

Valentina Parisi, Giuseppe Rengo, Pasquale Perrone-Filardi, Gennaro Pagano, Grazia Daniela Femminella, Stefania Paolillo, Laura Petraglia, Giuseppina Gambino, Aurelio Caruso, Maria Gabriella Grimaldi, Francesco Baldascino, Maria Nolano, Andrea Elia, Alessandro Cannavo, Antonio De Bellis, Enrico Coscioni, Teresa Pellegrino, Alberto Cuocolo, Nicola Ferrara, Dario Leosco

Rationale: **It has been reported that epicardial adipose tissue (EAT) may affect myocardial autonomic function.**

Objective: **The aim of this study was to explore the relationship between EAT and cardiac sympathetic nerve activity in patients with heart failure.**

Methods and Results: **In 110 patients with systolic heart failure, we evaluated the correlation between echocardiographic EAT thickness and cardiac adrenergic nerve activity assessed by ^{123}I-metaiodobenzylguanidine (^{123}I-MIBG). The predictive value of EAT thickness on cardiac sympathetic denervation (^{123}I-MIBG early and late heart:mediastinum ratio and single-photon emission computed tomography total defect score) was tested in a multivariate analysis. Furthermore, catecholamine levels, catecholamine biosynthetic enzymes, and sympathetic nerve fibers were measured in EAT and subcutaneous adipose tissue biopsies obtained from patients with heart failure who underwent cardiac surgery. EAT thickness correlated with ^{123}I-MIBG early and late heart:mediastinum ratio and single-photon emission computed tomography total defect score, but not with left ventricular ejection fraction. Moreover, EAT resulted as an independent predictor of ^{123}I-MIBG early and late heart:mediastinum ratio and single-photon emission computed tomography total defect score and showed a significant additive predictive value on ^{123}I-MIBG planar and single-photon emission computed tomography results over demographic and clinical data. Although no differences were found in sympathetic innervation between EAT and subcutaneous adipose tissue, EAT showed an enhanced adrenergic activity demonstrated by the increased catecholamine levels and expression of catecholamine biosynthetic enzymes.**

Conclusions: **This study provides the first evidence of a direct correlation between increased EAT thickness and cardiac sympathetic denervation in heart failure. (*Circ Res*. 2016;118:1244-1253. DOI: 10.1161/CIRCRESAHA.115.307765.)**

Key Words: echocardiography ■ epicardial adipose tissue ■ heart failure ■ MIBG ■ nuclear radiology ■ sympathetic nervous system

Cardiac sympathetic nervous system (SNS) hyperactivity is a specific hallmark of heart failure (HF)[1–6] and represents a compensatory response in the initial phase of this syndrome aimed at enhancing myocardial inotropism and preserving cardiac output. However, in the long term, this mechanism promotes maladaptive cardiac remodeling, life-threatening ventricular arrhythmias, worsening symptoms, and increased mortality.[1–6] In the failing heart, a defect of neuronal norepinephrine reuptake caused by post-transcriptional downregulation of the cardiac norepinephrine transporter[7–11] leads to an increase in norepinephrine concentration in the sympathetic synapses. This is responsible for impaired myocardial β-adrenergic receptor system and functional and anatomic sympathetic denervation of the heart.[12,13]

In This Issue, see p 1185
Editorial, see p 1189

Original received October 5, 2015; revision received February 25, 2016; accepted February 26, 2016. In January 2016, the average time from submission to first decision for all original research papers submitted to *Circulation Research* was 14.92 days.

From the Department of Translational Medical Sciences (V.P., G.R., G.P., G.D.F., L.P., G.G., A.C., N.F., D.L.) and Department of Advanced Biomedical Science (P.P.-F., T.P., A.C.), University Federico II, Naples, Italy; Department of Cardiology (G.R., G.G.) and Department of Neurology (M.N., A.E.), Salvatore Maugeri Foundation, IRCCS, Istituto di Telese, Benevento, Italy (G.R., G.G., M.N., A.E.); SDN Foundation, Institute of Diagnostic and Nuclear Development, Naples, Italy (S.P.); Department of Cardiology and Cardiac Surgery, Casa di Cura San Michele, Maddaloni (CE), Italy (A.C., M.G.G., F.B., A.D.B.); Department of Cardiac Surgery, Ruggi D'Aragona Hospital, Salerno, Italy (E.C.); and Institute of Biostructure and Bioimaging Italian National Research Council (CNR), Naples, Italy (T.P.).

The online-only Data Supplement is available with this article at http://circres.ahajournals.org/lookup/suppl/doi:10.1161/CIRCRESAHA.115.307765/-/DC1.

Correspondence to Giuseppe Rengo, MD, PhD, Department of Translational Medical Sciences, University Federico II, Via S. Pansini 5, 80131 Naples, Italy. E-mail giuseppe.rengo@unina.it

Nonstandard Abbreviations and Acronyms

EAT	epicardial adipose tissue
H/M	heart:mediastinum
HF	heart failure
HRV	heart rate variability
^{123}I-MIBG	^{123}I-metaiodobenzylguanidine
LV	left ventricular
LVEF	left ventricular ejection fraction
NYHA	New York Heart Association
SCAT	subcutaneous adipose tissue
SNS	sympathetic nervous system
TDS	total defect score

Furthermore, experimental studies in severe HF animals have demonstrated that prolonged exposure of high plasma norepinephrine concentration causes reduced myocardial expression of neurotrophic factors such as the nerve growth factor, thus resulting in cardiac sympathetic fiber loss.[14] Although it is widely recognized that cardiac SNS hyperactivity in HF is mainly mediated by norepinephrine-releasing neurons and by circulating norepinephrine and epinephrine, other mechanisms may contribute to SNS hyperactivation. For example, the adipose tissue, particularly the visceral fat depots, may stimulate central SNS activity through dysregulated adipokine production and secretion.[15–17] In addition, experimental studies have recently demonstrated that adipocytes produce and secrete both norepinephrine and epinephrine,[18] therefore, suggesting that the sympathetic fibers within adipose tissue are not the only source of catecholamines. Epicardial adipose tissue (EAT) is the visceral fat depot of the heart and represents a source of several adipocytokines and other bioactive molecules.[19,20] Because of its proximity to the myocardium and absence of fascial boundaries, EAT directly influences myocardial homeostasis through vasocrine and paracrine mechanisms. In fact, abnormalities of EAT secretory properties are implicated in the development of pathological conditions, including coronary atherosclerosis, left ventricular (LV) hypertrophy, LV diastolic dysfunction, and aortic stenosis.[20–26] Moreover, EAT contains abundant adrenergic and cholinergic nerves that interact with the extrinsic nervous system.

The relationship between EAT and cardiac SNS activity in HF has not been adequately explored yet. Therefore, in the present study, we have investigated the correlation between EAT and cardiac adrenergic nerve activity in patients with HF caused by LV systolic dysfunction.

Methods

Study Population

The patient population included 110 consecutive patients with HF caused by ischemic and nonischemic causes enrolled between January 2013 and November 2014 at the HF clinic of Federico II University of Naples. All patients were clinically referred to cardioverter defibrillator implantation, as indicated for either primary or secondary prevention. Before cardioverter defibrillator implantation and within 7 days from enrollment, patients underwent ^{123}I-metaiodobenzylguanidine (^{123}I-MIBG) planar and single-photon emission computed tomography (SPECT) imaging and a 2D-echocardiographic study. We used the following inclusion criteria: (1) left ventricular ejection fraction (LVEF) ≤50% during optimized medical therapy; (2) stable hemodynamic conditions; (3) no acute coronary syndromes in the past 6 months. We excluded patients with hemodynamic instability, moderate to severe valvular disease, atrial fibrillation or flutter, ventricular paced rhythm, myocardial inflammatory diseases, and suboptimal echocardiographic image quality. At the time of enrollment, all patients underwent a complete clinical examination and blood withdrawal for routine biochemical determinations. Demographic data including age, sex, HF medications, cardiovascular risk factors and the presence of comorbidities were also collected. We also included a group of 44 healthy subjects matched for age (66.8±12.5), sex (male, 85%), and body mass index (26.5±1.7). In these control subjects, we excluded the presence of cardiovascular diseases, cardiovascular risk factors, renal diseases, systemic inflammatory diseases, or any cardiovascular drug therapy. This group served as a control for echocardiographic EAT thickness comparisons. The study was approved by the local Ethics Committee. All procedures performed in the study were in accordance with the ethical standards of the institutional or national research committee and with the 1964 Helsinki declaration and its later amendments or comparable ethical standards and conformed to the Declaration of Helsinki on human research. All patients included in the study gave written informed consent after receiving an accurate explanation of the study protocol and of the potential risks related to the procedures adopted by the study.

Echocardiographic Study

Echocardiograms were performed by a VIVID E9 (GE Healthcare) machine, according to standard techniques. Echocardiographic images were recorded through an EchoPAC Clinical Workstation Software (GE Healthcare).

In all HF patients and in control subjects, measurements of EAT thickness were obtained from a parasternal long-axis view. EAT thickness was measured at end systole, perpendicularly to the free wall of the right ventricle in 3 cardiac cycles as previously described by Iacobellis and Willens.[27] Measurements of EAT thickness were performed offline by 2 independent operators. The average value from 3 cardiac cycles was used for the statistical analysis. The intraobserver and interobserver correlation coefficients were tested.

^{123}I-MIBG Myocardial Scintigraphy

All patients with HF underwent planar and SPECT ^{123}I-MIBG cardiac imaging according to the recommendations of the EANM Cardiovascular Committee and the European Council of Nuclear Cardiology,[28] as previously described in detail.[29] We also included data from a control group of 10 subjects who underwent cardiac ^{123}I-MIBG scintigraphy to rule out a disease of the adrenal medulla. An activity of 111 MBq ^{123}I-MIBG (Covidien, Mallinckrodt) was intravenously administered >1 to 2 minutes after thyroid blockade by oral administration of 300 mg of potassium perchlorate. Ten-minute planar images of the thorax in standard anterior view (256×256 matrix) were performed 15 minutes (early image) and 3 hours and 50 minutes (late image) after tracer administration. Four hours after tracer administration, a SPECT study (step and shoot mode, 90 projections, imaging time 30 minutes, 64×64 matrix) was performed. Imaging was performed using a dual-head camera system (Skylight, Philips) equipped with a low-energy, parallel-hole, high-resolution collimator, and the camera peaked at 159 keV with a symmetrical 20% energy window. From planar images, the heart:mediastinum (H/M) ratio was computed by dividing the mean counts per pixel within the myocardium by the mean counts per pixel within the mediastinum. Using dedicated postprocessing software on a dedicated workstation (Philips), the cardiac region of interest for assessment was polygonal in shape and drawn manually over the myocardium including the LV cavity on the planar MIBG images. Care was taken to exclude lung and liver from the myocardial region of interest. The mediastinal region of interest with a square shape was placed on the upper half of the mediastinum and had a size of 7×7 pixels. The location of the mediastinal region of interest was determined using as landmarks the lung apex, the upper cardiac border and the medial contours of the lungs. H/M ratios were computed for early and late planar imaging by dividing the mean counts per pixel within the myocardium by the mean counts per pixel within the mediastinum. The MIBG washout

rate was calculated using the following formula: ([early heart counts per pixel−early mediastinum counts per pixel]−[late heart counts per pixel decay-corrected−late mediastinum counts per pixel decay corrected])/(early heart counts per pixel−early mediastinum counts per pixel)×100. SPECT studies were processed with filtered back-projection and reconstructed into standard long-axis and short-axis images, perpendicular to the heart axis. From SPECT images, the defect score was calculated by assessing the patient's segmental tracer uptake score using the 17-segment model.[30] Each myocardial segment was scored according to the following tracer uptake scale: 0 normal, 1 mildly reduced, 2 moderately reduced, 3 severely reduced, and 4 no uptake. The total defect score (TDS) was calculated as the sum of the segmental tracer uptake scores (summed score) and separately for each vascular territory. Images interpretation was done by consensus of 2 independent readers. Intra- and interobserver reproducibility was excellent, thus confirming our recent results from a low-dose MIBG cardiac imaging protocol in patients with HF.[29] No patient was excluded for poor quality of MIBG images.

Heart Rate Variability Analysis of Cardiac Parasympathetic Activity

Heart rate variability (HRV) was assessed from 24-hour ambulatory Holter ECG monitoring (Mars System; GE Healthcare). To evaluate cardiac parasympathetic activity, we used the root-mean-square of the successive normal sinus RR interval difference and the percentage of successive normal sinus RR intervals >50 ms (pNN50) in the time domain HRV, and the high-frequency oscillation in the spectral HRV domain.

Tissues Collection and Norepinephrine and Epinephrine Determination

Of 110 patients with HF enrolled into the study, 16 underwent cardiac surgery for coronary artery bypass grafting. From this group of patients, we obtained EAT and subcutaneous adipose tissue (SCAT) samples during cardiac intervention. EAT and SCAT biopsy samples (average 0.1–0.5 g) were obtained before the initiation of cardiopulmonary bypass. EAT biopsies were taken near the proximal right coronary artery, whereas SCAT samples were obtained from the chest. Tissue sample were homogenized with tissue homogenizer (Ultra-Turrax, IKA T10) in 1 mL of 0.01 mol/L HCl, 1 mmol/L EDTA, and 4 mmol/L sodium metabisulfite, stored in ice for 1 hour, and centrifuged for 15 minutes (13 100*g*, 4°C), the supernatants were used for the catecholamines determination by enzyme immunoassay.

Norepinephrine and epinephrine were measured in EAT, SCAT, and plasma. All measurements were performed using 2-CAT Research RIA kits (Labor Diagnostika Nord, Nordhorn, Germany) according to the manufacturer's protocol.

RNA Isolation and Absolute Quantification of Tyrosine Hydroxylase, Dopamine-β-Hydroxylase, and Phenylethanolamine N-Methyltransferase mRNA Levels by Real-Time Polymerase Chain Reaction Using SYBR Green

Total RNA was isolated from EAT and SCAT samples with RNasy Lipid Tissue Mini Kit (Qiagen) according to the manufacturer's instructions. The purity and concentration of isolated RNA were measured with NanoDrop (Jenway, Genova Nano). Reverse transcription was performed in 20 μL of reaction mixture containing 180 ng of total RNA, with High Capacity cDNA Reverse Transcription kits (Applied Biosystems) according to the manufacturer's protocol. Absolute mRNA levels of tyrosine hydroxylase (TH), dopamine-β-hydroxylase (DBH), and phenylethanolamine N-methyltransferase (PNMT) were evaluated by quantitative real-time polymerase chain reaction on thermocycler iQ5 Multicolor (Bio-Rad). The amounts of mRNA were determined by amplification of 18 ng of cDNA target using iQ SYBR Green Supermix (Bio-Rad) according to manufacturer's protocols. Reactions also contained 300 nmol each of the forward and reverse primers: PNMT forward primer, 59-GCA GCC ACT TTG AGG ACA TCA-39; PNMT reverse primer, 59-GGC TGT ACA TGC TCC AGT TGA A-39; TH forward primer, 59-CGG ATG AGG AAA TTG AGA AGC T-39; TH reverse primer, 59-TCT GCT TAC ACA GCC CGA ACT-59; DBH forward primer 5′-GTGCTACATTAAGGAGCTTCCAAAG-3′), reverse primer 5′-GGCCTCATTGCCCTTGGT-3′. GAPDH rRNA was used as endogenous control.

Real-time polymerase chain reaction conditions were a typical 2-step real-time polymerase chain reaction protocol, 2 minutes at 95°C, followed by 40 cycles of denaturation for 15 seconds at 95°C and annealing/extension for 30 seconds at 60°C. The polymerase chain reaction products were quantified with an automatic sequence detection system at each step of amplification using the Optical System Software (version 2.1; Bio-Rad).

Immunoblotting

SCAT and EAT samples were weighed (≈15 mg) and lysed in 150 μL of RIPA buffer with protease and phosphatase inhibitors cocktail (Roche). Protein concentrations in all lysates were measured using a dye-binding protein assay kit (Bio-Rad) and a spectrophotometer reader (Bio-Rad) at a wavelength of 750 nm. Protein levels of TH were detected by protein immunoblotting using a 1:1000 anti-rabbit IgG (Millipore AB152); PNMT was detected using 1:1000 anti-mouse IgG (WH0005409M6; Sigma); GAPDH was used as internal loading control. Secondary antibodies were purchased from ImmunoReagents, Inc., Raleigh. Bands were visualized by enhanced chemiluminescence (ECL; Millipore Immobilon, Western Chemiluminescent HRP Substrate) and were quantified using densitometry (Chemidoc; Bio-Rad).

Immunohistochemical Procedures

EAT and SCAT samples were frozen at −80°C and cut in 50-μm consecutive thick sections using a freezing microtome (Leica 2000R, Germany). Free-floating sections were processed by means of indirect immunofluorescence technique using rabbit polyclonal antibodies against TH (Millipore AB152, 1:1000) to mark sympathetic nerve fibers. In both EAT and SCAT, most of the sympathetic nerve fibers were localized along vessels with few scattered fibers randomly distributed. Therefore, to quantify vascular innervation, digital images of all vessels found in 42 stained sections were acquired using nonlaser confocal microscopy (Apotome confocal system; Zeiss, Oberkochen, Germany). The highest number of fibers running along the vessel and intercepting a superimposed line perpendicular to the major axis of the vascular structure were counted. We measured the total number of intercepts for each vessel and the nerve density calculated as the mean number of intercepts per vessel caliber in μm (fibers/μm). A single operator blindly performed all the measurements.

Statistical Analysis

Continuous variables were expressed as mean±SD and compared by the use of Student *t* test (normally distributed) or as median±interquartile range value and compared by the use of Mann–Whitney *U* test (not normally distributed), as appropriate. Normality of data distribution was evaluated using the Kolmogorov–Smirnov test. Categorical variables were expressed as proportion and compared by use of χ^2 test. Pearson correlation coefficient was calculated to assess correlation between data. To determine the independent predictors of ^{123}I-MIBG early and late H/M, and late SPECT, variables achieving $P<0.10$ on univariate analysis (age, sex, LVEF, New York Heart Association [NYHA] class, body mass index, ischemic versus non ischemic HF cause, diabetes mellitus, hypertension, dyslipidemia, and EAT thickness) were then included in a multivariate linear regression analysis. The additive predictive value of EAT thickness on ^{123}I-MIBG planar and SPECT results was assessed by the increase of r^2 in a 3-step linear regression modeling. The first step consisted of fitting a multivariate model 1 of age, sex, NYHA class, HF of ischemic cause, diabetes mellitus, hypertension, and dyslipidemia. Then, LVEF was included in the second step. Next, EAT thickness was included in the third step. The change in overall r^2 was used to assess the increase in predictive power after the addition of each variable. All data were collected in an Excel database and analyzed by SPSS version 19.0 (SPSS, Inc., Chicago, IL). Statistical significance was accepted at $P<0.05$.

Results

Patient Characteristics

Table 1 illustrates demographic, clinical, echocardiographic, and ^{123}I-MIBG characteristics of the HF population. The mean age was 64.74±10.50 years and 85.5% of patients were men. The majority of the patients were in NYHA class II (60%) and III (36.4%). Ischemic cause of HF was recognized in 72% of cases. Forty-two percent of the patients were diabetics, 74% had hypertension, 45% were smokers, and 72% had dyslipidemia. The majority of the patients were on optimal HF drug therapy. Mean LVEF was 38.1±9.3%, and mean EAT thickness was 8.6±2.55 mm. At ^{123}I-MIBG scintigraphy, mean early and late H/M were significantly lower than in healthy controls (early H/M, 1.76±0.23 versus 2.23±0.18; P<0.0001; late H/M, 1.57±0.25 versus 2.14±0.19; P<0.0001; Online Figure I). In the patients with HF, the washout rate was 10.83±10.04, and the mean SPECT TDS was 35.6±16.8. Overall, these data are consistent with cut-off data previously reported by our group and others[10,11] and indicate a significant cardiac sympathetic denervation. In patients with HF, the EAT thickness value was significantly higher than in controls (8.6±2.55 versus 4.7±1.24 mm; P<0.001), which is consistent with the increase in LV end-diastolic mass (202±48 versus 122±26 g; P<0.01).[24] The reproducibility for echocardiographic EAT thickness assessment was excellent (intraobserver, 0.897; interobserver, 0.921).

Table 1. Demographic and Clinical Characteristics of the Study HF Population

	All (n=110)
Age, y	64.74±10.50
Sex, male, % (n)	85.5 (94)
BMI, kg/m^2	28.6±4.4
NYHA class, % (n)	
I	3.6 (4)
II	60 (66)
III	36.4 (40)
HF ischemic cause, % (n)	71.8 (79)
Family history of CAD, % (n)	24.5 (27)
Diabetes mellitus, % (n)	41.8 (46)
Hypertension, % (n)	74.5 (82)
Smokers, % (n)	45.5 (50)
Dyslipidemia, % (n)	71.8 (79)
CKD, % (n)	15.5 (17)
COPD, % (n)	32.7 (36)
Cardiac drug therapy, % (n)	
ACE-I/ARBs	80.9 (89)
MRA antagonist	43.6 (48)
CCBs	10.0 (11)
BBs	75.5 (83)
Echocardiographic data	
EAT thickness, mm	8.6±2.55
LVEF, %	38.1±9.3
LV-EDM, g	202±48
^{123}I-MIBG myocardial scintigraphy	
Early H/M	1.76±0.23
Late H/M	1.57±0.25
Washout rate	10.83±10.04
SPECT TDS	35.6±16.8

ACE-I indicates angiotensin-converting enzyme inhibitors; ARB, angiotensin receptor blockers; BB, β-blockers; BMI, body mass index; CAD, coronary artery disease; CCB, calcium channel blockers; CKD, chronic kidney disease; COPD, chronic obstructive pulmonary disease; EAT, epicardial adipose tissue; H/M, heart:mediastinum ratio; HF, heart failure; ^{123}I-MIBG, iodine-123 meta-iodobenzylguanidine; LV-EDM, left ventricular end-diastolic mass; LVEF, left ventricular ejection fraction; MRA, mineralcorticoid antagonists; NYHA, New York Heart Association; SPECT, single-photon emission computed tomography; and TDS, total defect score.

Correlation Between Echocardiographic EAT Thickness and Cardiac ^{123}I-MIBG Data: Multivariable Predictors of Cardiac Sympathetic Denervation

EAT thickness showed a weak, although significant, correlation with planar ^{123}I-MIBG parameters (early and late H/M), whereas a more evident correlation was found with ^{123}I-MIBG SPECT TDS (Figure 1; Online Table I). There was no correlation between EAT and LVEF (Online Table I). Noteworthy, LVEF significantly correlated with late H/M (r = 0.388; P<0.0001), but not with early H/M, washout rate and SPECT TDS (Online Table II).

Multivariate linear regression analyses were used to assess the predictors of ^{123}I-MIBG planar and SPECT parameters (Table 2). The EAT thickness resulted as a significant independent predictor of ^{123}I-MIBG early and late H/M, and SPECT TDS. LVEF and NYHA class significantly predicted both early and late H/M, but not SPECT TDS. The incremental predictive value of EAT thickness on ^{123}I-MIBG planar and SPECT parameters was evaluated from the increase of r^2 in a 3-step linear regression modeling (Figure 2). For ^{123}I-MIBG SPECT TDS (Figure 2A), early (Figure 2B), and late H/M (Figure 2C), the addition of EAT thickness significantly increased global r^2 (P<0.05) over model 1 (including age, sex, body mass index, NYHA class, HF of ischemic cause, diabetes mellitus, hypertension, and dyslipidemia) plus LVEF.

EAT Thickness, Cardiac Sympathetic Denervation, and LV Mass

LV mass significantly correlated with both EAT thickness and cardiac sympathetic denervation expressed by ^{123}I-MIBG late H/M (Figure 3). The significant correlation between EAT and ^{123}I-MIBG late H/M is illustrated in Figure 1.

Catecholamine Concentration, Catecholamine Biosynthetic Enzymes, and Sympathetic Innervation in EAT and SCAT

EAT and SCAT from patients with HF contained both norepinephrine and epinephrine. More important, EAT showed a 5.6-fold increase of norepinephrine levels when compared with SCAT (0.168±0.026 versus 0.030±0.008 ng/

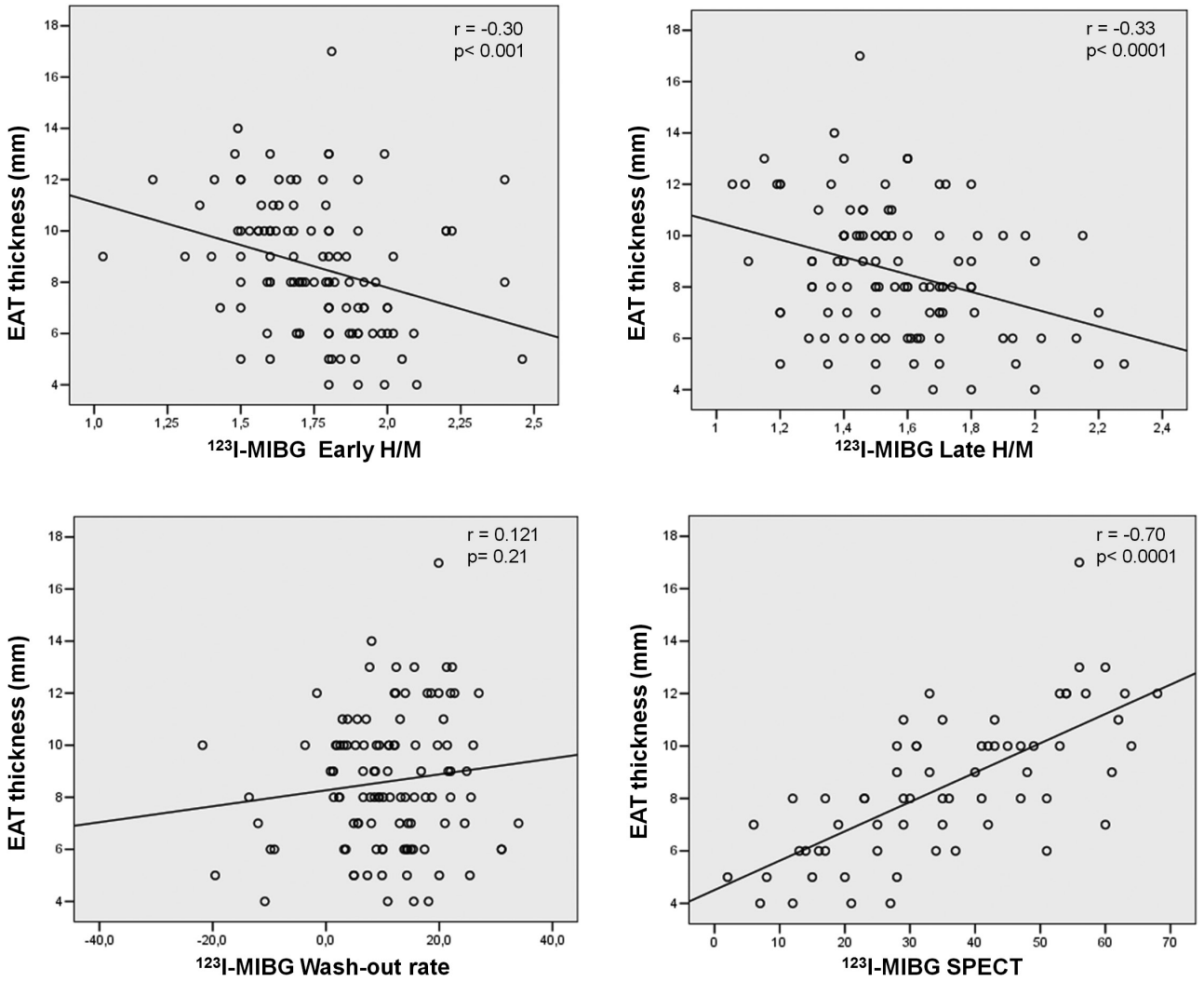

Figure 1. Correlation between epicardial adipose tissue (EAT) thickness and planar (early and late heart:mediastinum ratio [H/M]; washout rate) and single-photon emission computed tomography (SPECT) data at cardiac ^{123}I-metaiodobenzylguanidine (^{123}I-MIBG) imaging.

mL; *P*<0.0001) and a 2-fold increase when compared with plasma (0.168±0.026 versus 0.085±0.014 ng/mL; *P*=0.017; Figure 4A). Epinephrine levels were significantly higher in EAT than in SCAT (0.016±0.001 versus 0.008±0.0005 ng/mL; *P*<0.0001), but lower than in plasma (0.016±0.001 versus 0.06±0.008 ng/mL; *P*<0.0001; Figure 4A).

We investigated whether norepinephrine and epinephrine were produced in adipose tissues. Gene expression of all catecholamine biosynthetic enzymes (TH, DBH, and PNMT) was evident in both EAT and SCAT. mRNA levels of norepinephrine-synthesizing enzymes (TH and DBH) were significantly higher in EAT than in SCAT (8.6-fold and 6.5-fold increase, respectively), which explained the higher norepinephrine concentrations in EAT (Figure 4B). We observed a robust increase of both TH and PNMT protein levels in EAT when compared with protein levels in SCAT (Figure 4C). The increased protein expression of PNMT in EAT when compared with SCAT was not paralleled by a similar (statistically significant) increase at the mRNA level. We quantified sympathetic nerve fibers in a total number of 45 vessels. We did not find differences in the mean number of fibers per vessel between EAT and SCAT (Figure 4D). On the contrary, the mean vessel diameter in EAT was significantly higher than SCAT vessel diameter (100.37±53.35 and 58.76±30.64 μm, respectively; *P*<0.001). Therefore, the fiber density per vessel diameter was significantly higher in SCAT than in EAT (*P*<0.001; Figure 4D). Taken together, these data indicate a higher SNS activation in EAT than in SCAT in our HF population.

EAT and Cardiac Parasympathetic Activity

HRV data of cardiac parasympathetic activity in patients with HF are reported in Online Table III.

Because our evidence indicated a correlation between EAT thickness and cardiac sympathetic nerve derangement, we also explored the relationship between EAT thickness and HRV measures of cardiac parasympathetic activity. In our HF population, EAT thickness did not correlate with pNN50 (Pearson = 0.102; *P*=0.67), root-mean-square of the successive normal sinus RR interval difference (Pearson = 0.079; *P*=0.74), and high-frequency oscillation (Pearson= 0.051; *P*=0.83; Online Table IV).

Table 2. Multivariable Predictors of ^{123}I-MIBG Planar and SPECT Data

	β	Lower 95% CI	Upper 95% CI	*P* Value
^{123}I-MIBG early H/M				
Age	−0.001	−0.006	0.004	0.568
Sex	−0.083	−0.226	0.059	0.269
BMI	−0.012	−0.025	0.0002	0.159
NYHA	−0.119	−0.202	−0.035	0.006
HF ischemic cause	0.009	−0.056	0.076	0.768
Diabetes mellitus	0.018	−0.066	0.104	0.688
Hypertension	0.084	−0.032	0.202	0.236
Dyslipidemia	−0.039	−0.153	0.074	0.594
LVEF	0.005	0.0006	0.011	0.002
EAT thickness	−0.030	−0.048	−0.012	0.001
^{123}I-MIBG late H/M				
Age	−0.005	−0.010	0.0002	0.053
Sex	−0.073	−0.217	0.071	0.398
BMI	−0.004	−0.017	0.009	0.522
NYHA	−0.162	−0.248	−0.075	0.000
HF ischemic cause	0.029	−0.037	0.096	0.353
Diabetes mellitus	−0.031	−0.117	0.055	0.431
Hypertension	0.128	0.010	0.247	0.082
Dyslipidemia	−0.010	−0.125	0.104	0.858
LVEF	0.007	0.002	0.012	0.009
EAT thickness	−0.034	−0.052	−0.014	0.001
^{123}I-MIBG SPECT TDS				
Age, y	0.130	−0.281	0.542	0.592
Sex	−6.342	−17.779	5.095	0.402
BMI	−0.420	−1.456	0.615	0.434
NYHA	1.719	−4.661	8.100	0.341
HF ischemic cause	4.340	−3.042	11.723	0.580
Diabetes mellitus	1.503	−5.022	8.029	0.645
Hypertension	3.455	−5.122	12.033	0.465
Dyslipidemia	4.850	−4.552	14.252	0.412
LVEF	−0.452	−0.877	−0.027	0.072
EAT thickness	4.392	3.169	5.614	0.000

BMI indicates body mass index; CI, confidence interval; EAT, epicardial adipose tissue; H/M, heart:mediastinum ratio; HF, heart failure; ^{123}I-MIBG, iodine-123 meta-iodobenzylguanidine; LVEF, left ventricular ejection fraction; NYHA, New York Heart Association; and TDS, total defect score.

Discussion

The findings of the present study, obtained in patients with systolic HF, demonstrate that a highly significant correlation exists between EAT thickness and cardiac sympathetic denervation assessed by cardiac ^{123}I-MIBG; furthermore, EAT thickness predicts cardiac ^{123}I-MIBG planar and SPECT parameters, incrementally to clinical and LV function data. Finally, EAT represents an important source of catecholamines in patients with HF.

EAT and Cardiac Sympathetic Denervation

EAT represents the visceral fat depot of the heart which covers 80% of the heart's surface and constitutes 20% of its total weight.[20] It is known that in pathological conditions, EAT may play an unfavorable activity for the heart through production and secretion of proinflammatory and proatherogenic factors.[19–21] Importantly, recent studies have also indicated a close relationship between EAT and myocardial autonomic function.[31,32] Many EAT-derived factors can directly modulate the electrophysiological properties and ion currents of myocytes and may promote arrhythmogenesis.[33] Moreover, EAT contains both adrenergic and cholinergic nerves which interact with the extrinsic SNS and para-SNS.[34,35] Simultaneous activation of these nerve structures within EAT in response to extrinsic nerve activation may enhance triggered activity and facilitate the development of cardiac arrhythmias.[32] In this study, we have demonstrated that EAT represents an important source of norepinephrine, whose levels are 2-fold higher than those found in plasma. Because of the EAT proximity to the myocardium, the increase in catecholamine content in this tissue could result in a negative feedback on cardiac sympathetic nerves, which are associated with the ventricular myocardium, thus inducing a functional and anatomic denervation of the heart. This hypothesis is supported by our findings showing a direct correlation between EAT thickness and the degree of cardiac sympathetic denervation assessed by cardiac ^{123}I-MIBG. Therefore, in the context of a widespread SNS hyperactivity in HF, EAT seems to play an additive role in generating the final net effect of cardiac sympathetic denervation. In fact, when the failing myocardium shows depletion of norepinephrine stores because of reduced mechanisms of norepinephrine uptake,[7] circulating catecholamines derived from peripheral organs might play a prominent role in perpetuating the progression of cardiac sympathetic denervation. This is particularly relevant given the importance of cardiac sympathetic nerves in cardiac homeostasis[36] and repair.[37] In this regard, it has been demonstrated that cardiac chemical sympathectomy in rats induces LV contractility dysfunction, increased circulating levels of markers of severe myocardial damage, and cardiac inflammatory reactions.[36] In addition, sympathetic denervation completely blocks cardiac regenerative responses after injury in neonatal hearts.[37]

In our analysis, the EAT thickness was an independent predictor of ^{123}I-MIBG planar and SPECT parameters and provided additional predictive information on cardiac adrenergic nerve activity respect to important demographic, clinical, and LV function parameters. Therefore, assessing EAT thickness in patients with HF may provide surrogate information on the status of cardiac adrenergic derangement, independently from the degree of LV systolic dysfunction and clinical variables. On the contrary, the increase in SNS activity in the EAT did not show any effect on cardiac parasympathetic activity. In this regard, the interaction between cardiac sympathetic and parasympathetic innervation and its effect on cardiac parasympathetic activity has been largely unexplored. The evidence comes only from few experimental studies conducted

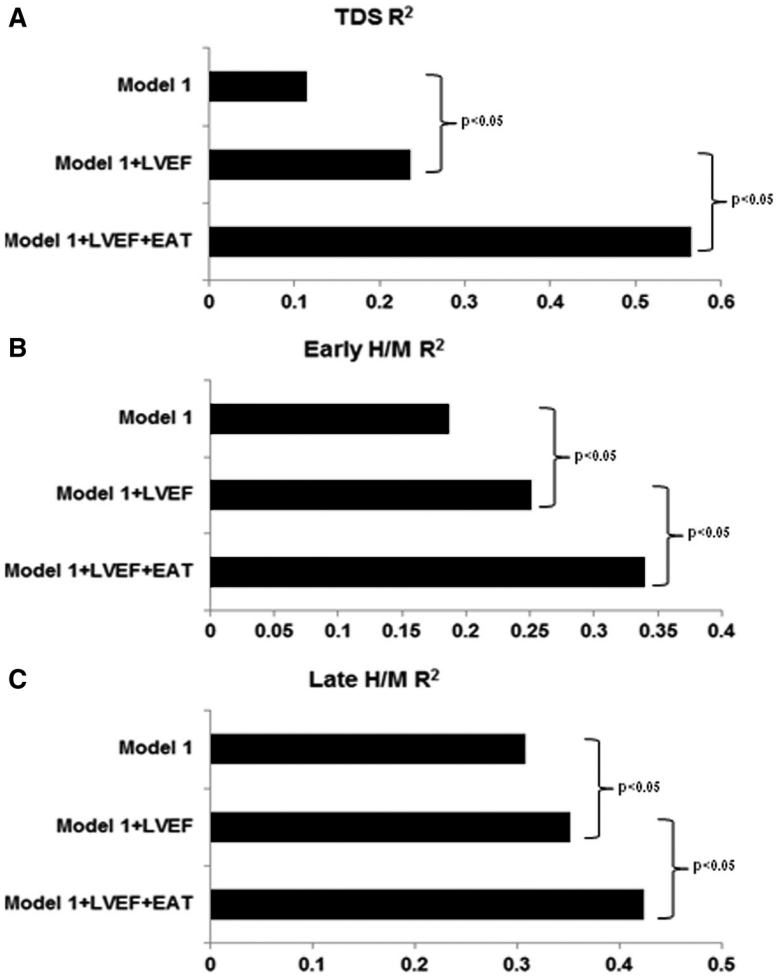

Figure 2. Additive predictive value of epicardial adipose tissue (EAT) thickness on ^{123}I-metaiodobenzylguanidine single-photon emission computed tomography total defect score (TDS) (A) and planar (early [B] and late [C] heart:mediastinum ratio [H/M], assessed by the increase of r^2 in a 3-step linear regression modeling. The first step consisted of fitting a multivariate model 1 of age, gender, body mass index, New York Heart Association class, heart failure of ischemic cause, diabetes, hypertension and dyslipidemia. Left ventricular ejection fraction (LVEF) was included in the second step (model 1+LVEF). EAT thickness was included in the third step. The change in overall r^2 was used to assess the increase in predictive power after the addition of each variable.

in non-HF animal models,[36] thus avoiding comparisons with our results obtained in the clinical setting.

Overall, these findings seem particularly relevant given the well-recognized importance to assess cardiac sympathetic denervation for the prognostic stratification of patients with advanced HF.[11]

In our patients with HF, the EAT thickness value was significantly higher than in controls consistent with the increase in LV end-diastolic mass.[24,38] Interestingly, according to previous evidence reporting a relationship between LV hypertrophy and cardiac sympathetic denervation in hypertensive patients,[39] our data indicate a close relationship between EAT,

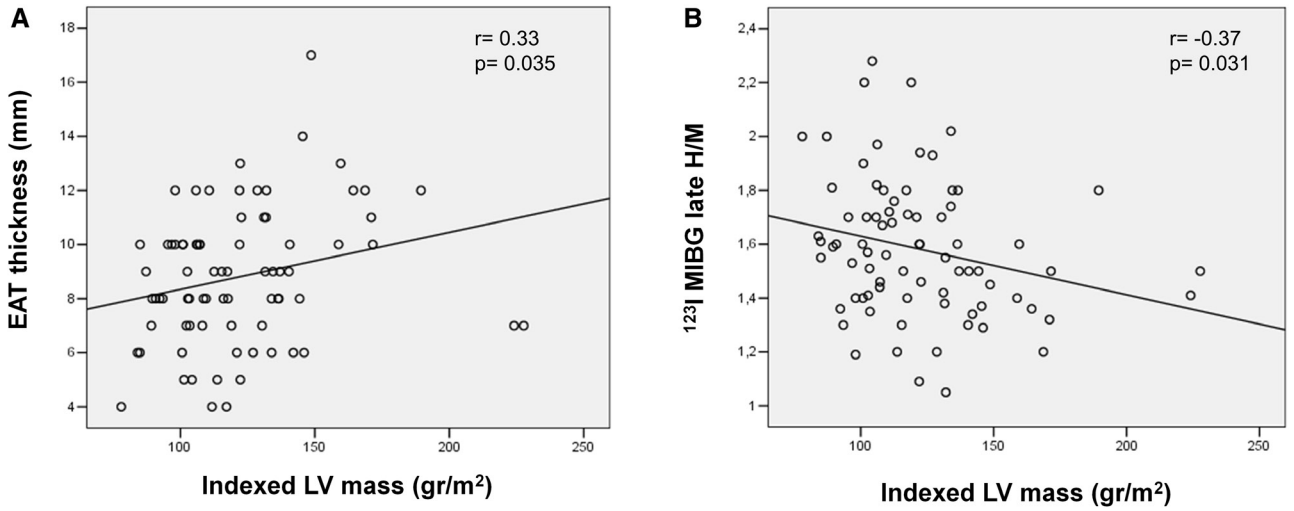

Figure 3. A, Correlation between epicardial adipose tissue (EAT) thickness and indexed left ventricular (LV) mass. B, Correlation between ^{123}I-metaiodobenzylguanidine (^{123}I-MIBG) late heart:mediastinum (H/M) ratio and indexed LV mass.

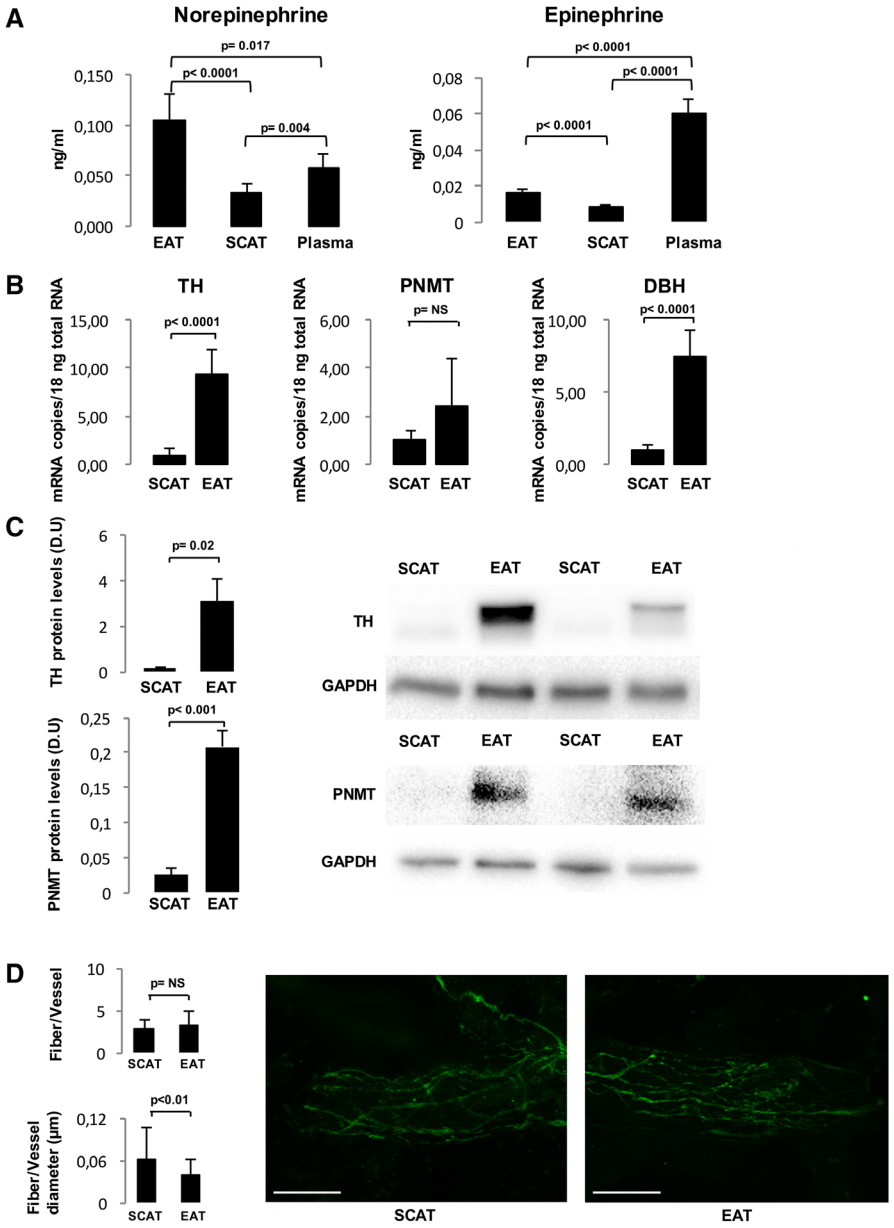

Figure 4. A, Norepinephrine and epinephrine determination by enzyme immunoassay in epicardial adipose tissue (EAT), subcutaneous adipose tissue (SCAT), and plasma of patients with heart failure. **B**, Quantification of tyrosine hydroxylase (TH), dopamine-β-hydroxylase (DBH), and phenylethanolamine N-methyltransferase (PNMT) mRNA levels by real-time polymerase chain reaction in SCAT and EAT. **C**, Average densitometric quantitative analysis (**left**) and representative Western blot (**right**) from blots showing the ratio of TH and PNMT to GAPDH in SCAT and EAT. **D**, Sympathetic nerve fibers density in SCAT and EAT expressed as number of fibers per vessel and fiber per micrometer of vessel diameter (**left**) and representative confocal images (**right**) showing sympathetic nerve fibers along vessels in SCAT and EAT obtained from a patient with heart failure. Fibers are marked with TH antibodies. Scale bar, 50 µm in SCAT and 100 µm in EAT.

cardiac sympathetic denervation, and HF severity expressed by the increase of LV mass.

Catecholamine Production in EAT

Adipose tissues contain a rich sympathetic innervation.[40–42] Activation of fat sympathetic fibers leads to the release of catecholamines (mainly norepinephrine), which stimulate fat cell β1, β2, β3, and α2-adrenergic receptors; this mechanism activates or inhibits the lipolysis process.[42–46] Catecholamines are considered the major regulators of lipolysis[45,46] and also affect differentiation and proliferation of adipocytes.[47,48] Catecholamine biosynthesis is catalyzed primarily by TH, DBH, and PNMT enzymes,[49] and recent studies have indicated that the genes of these enzymes are differentially expressed in various adipose tissue depots.[18] The present study reports the first evidence of SNS activation in EAT of patients with HF. In fact, norepinephrine and epinephrine were both present in EAT; moreover, norepinephrine concentrations were higher than in SCAT and plasma. Accordingly, catecholamine signal transduction pathways were also found in EAT with a significant expression of genes (mRNA of TH, DBH, and PNMT) involved in the synthesis of norepinephrine and epinephrine. Notably, catecholamine levels and expression of the enzymes

involved in catecholamine biosynthesis were significantly higher in EAT than in SCAT. However, based on the histological analysis, SNS hyperactivity found in EAT was not associated with EAT hyperinnervation. These findings may explain, at least in part, the strong correlation between EAT thickness and ^{123}I-MIBG parameters observed in patients with HF. This supports the hypothesis that increased EAT directly contributes to SNS hyperactivity in the heart that accompanies and fosters myocardial sympathetic denervation and disease progression.

Limitations

The current study reports a single-center experience in a relatively small group of patients, and a mid-/long-term follow-up was not available for our study population.

Echocardiographic EAT measurement has several advantages, such as low cost and easy availability, but it also has some limitations because it might not fully reflect the variability of fat thickness or total EAT volume. However, the EAT echocardiographic evaluation has been reported to correlate with magnetic resonance measurements[27] and has an excellent reproducibility,[50] as confirmed in the current study.

The lack of a control group of patients without HF undergoing EAT and SCAT catecholamine measurements represents a limitation of the study. Another question could be raised on the influence of circulating catecholamines on the levels of norepinephrine and epinephrine in EAT and SCAT. However, norepinephrine levels in EAT were higher than in plasma, thus indicating a local production. Finally, the presence of genes of the catecholamine biosynthetic enzymes found in both EAT and SCAT points to an endogenous production of catecholamines in these adipose tissues.

Conclusions

In patients with HF, EAT independently correlates with cardiac sympathetic denervation and represents a source of catecholamine production. SNS activation in EAT might contribute to cardiac sympathetic denervation and disease progression in HF. These results pave the way for future evaluation on the potential use of EAT thickness as an index of cardiac adrenergic nerve activity and prognosis in patients with HF.

Disclosures

None.

References

1. Lymperopoulos A, Rengo G, Koch WJ. Adrenergic nervous system in heart failure: pathophysiology and therapy. *Circ Res*. 2013;113:739–753. doi: 10.1161/CIRCRESAHA.113.300308.
2. Rengo G, Lymperopoulos A, Koch WJ. Future G protein-coupled receptor targets for treatment of heart failure. *Curr Treat Options Cardiovasc Med*. 2009;11:328–338.
3. Triposkiadis F, Karayannis G, Giamouzis G, Skoularigis J, Louridas G, Butler J. The sympathetic nervous system in heart failure physiology, pathophysiology, and clinical implications. *J Am Coll Cardiol*. 2009;54:1747–1762. doi: 10.1016/j.jacc.2009.05.015.
4. Iaccarino G, Barbato E, Cipolletta E, De Amicis V, Margulies KB, Leosco D, Trimarco B, Koch WJ. Elevated myocardial and lymphocyte GRK2 expression and activity in human heart failure. *Eur Heart J*. 2005;26:1752–1758. doi: 10.1093/eurheartj/ehi429.
5. Rengo G, Perrone-Filardi P, Femminella GD, Liccardo D, Zincarelli C, de Lucia C, Pagano G, Marsico F, Lymperopoulos A, Leosco D. Targeting the β-adrenergic receptor system through G-protein-coupled receptor kinase 2: a new paradigm for therapy and prognostic evaluation in heart failure: from bench to bedside. *Circ Heart Fail*. 2012;5:385–391. doi: 10.1161/CIRCHEARTFAILURE.112.966895.
6. Rengo G, Lymperopoulos A, Leosco D, Koch WJ. GRK2 as a novel gene therapy target in heart failure. *J Mol Cell Cardiol*. 2011;50:785–792. doi: 10.1016/j.yjmcc.2010.08.014.
7. Böhm M, La Rosée K, Schwinger RH, Erdmann E. Evidence for reduction of norepinephrine uptake sites in the failing human heart. *J Am Coll Cardiol*. 1995;25:146–153.
8. Ungerer M, Hartmann F, Karoglan M, Chlistalla A, Ziegler S, Richardt G, Overbeck M, Meisner H, Schömig A, Schwaiger M. Regional in vivo and in vitro characterization of autonomic innervation in cardiomyopathic human heart. *Circulation*. 1998;97:174–180.
9. Backs J, Haunstetter A, Gerber SH, Metz J, Borst MM, Strasser RH, Kübler W, Haass M. The neuronal norepinephrine transporter in experimental heart failure: evidence for a posttranscriptional downregulation. *J Mol Cell Cardiol*. 2001;33:461–472. doi: 10.1006/jmcc.2000.1319.
10. Paolillo S, Rengo G, Pagano G, et al. Impact of diabetes on cardiac sympathetic innervation in patients with heart failure: a 123I meta-iodobenzylguanidine (123I MIBG) scintigraphic study. *Diabetes Care*. 2013;36:2395–2401. doi: 10.2337/dc12-2147.
11. Jacobson AF, Senior R, Cerqueira MD, Wong ND, Thomas GS, Lopez VA, Agostini D, Weiland F, Chandna H, Narula J; ADMIRE-HF Investigators. Myocardial iodine-123 meta-iodobenzylguanidine imaging and cardiac events in heart failure. Results of the prospective ADMIRE-HF (AdreView Myocardial Imaging for Risk Evaluation in Heart Failure) study. *J Am Coll Cardiol*. 2010;55:2212–2221. doi: 10.1016/j.jacc.2010.01.014.
12. Mardon K, Montagne O, Elbaz N, Malek Z, Syrota A, Dubois-Randé JL, Meignan M, Merlet P. Uptake-1 carrier downregulates in parallel with the beta-adrenergic receptor desensitization in rat hearts chronically exposed to high levels of circulating norepinephrine: implications for cardiac neuroimaging in human cardiomyopathies. *J Nucl Med*. 2003;44:1459–1466.
13. Bristow MR, Ginsburg R, Minobe W, Cubicciotti RS, Sageman WS, Lurie K, Billingham ME, Harrison DC, Stinson EB. Decreased catecholamine sensitivity and beta-adrenergic-receptor density in failing human hearts. *N Engl J Med*. 1982;307:205–211. doi: 10.1056/NEJM198207223070401.
14. Kimura K, Kanazawa H, Ieda M, Kawaguchi-Manabe H, Miyake Y, Yagi T, Arai T, Sano M, Fukuda K. Norepinephrine-induced nerve growth factor depletion causes cardiac sympathetic denervation in severe heart failure. *Auton Neurosci*. 2010;156:27–35. doi: 10.1016/j.autneu.2010.02.005.
15. Maffei M, Halaas J, Ravussin E, Pratley RE, Lee GH, Zhang Y, Fei H, Kim S, Lallone R, Ranganathan S. Leptin levels in human and rodent: measurement of plasma leptin and ob RNA in obese and weight-reduced subjects. *Nat Med*. 1995;1:1155–1161.
16. Considine RV, Sinha MK, Heiman ML, Kriauciunas A, Stephens TW, Nyce MR, Ohannesian JP, Marco CC, McKee LJ, Bauer TL. Serum immunoreactive-leptin concentrations in normal-weight and obese humans. *N Engl J Med*. 1996;334:292–295. doi: 10.1056/NEJM199602013340503.
17. Perrone-Filardi P, Paolillo S, Costanzo P, Savarese G, Trimarco B, Bonow RO. The role of metabolic syndrome in heart failure. *Eur Heart J*. 2015;36:2630–2634. doi: 10.1093/eurheartj/ehv350.
18. Vargovic P, Ukropec J, Laukova M, Cleary S, Manz B, Pacak K, Kvetnansky R. Adipocytes as a new source of catecholamine production. *FEBS Lett*. 2011;585:2279–2284. doi: 10.1016/j.febslet.2011.06.001.
19. Mazurek T, Zhang L, Zalewski A, Mannion JD, Diehl JT, Arafat H, Sarov-Blat L, O'Brien S, Keiper EA, Johnson AG, Martin J, Goldstein BJ, Shi Y. Human epicardial adipose tissue is a source of inflammatory mediators. *Circulation*. 2003;108:2460–2466. doi: 10.1161/01.CIR.0000099542.57313.C5.
20. Iacobellis G, Corradi D, Sharma AM. Epicardial adipose tissue: anatomic, biomolecular and clinical relationships with the heart. *Nat Clin Pract Cardiovasc Med*. 2005;2:536–543. doi: 10.1038/ncpcardio0319.
21. Baker AR, Silva NF, Quinn DW, Harte AL, Pagano D, Bonser RS, Kumar S, McTernan PG. Human epicardial adipose tissue expresses a pathogenic profile of adipocytokines in patients with cardiovascular disease. *Cardiovasc Diabetol*. 2006;5:1. doi: 10.1186/1475-2840-5-1.
22. Chaldakov GN, Stankulov IS, Aloe L. Subepicardial adipose tissue in human coronary atherosclerosis: another neglected phenomenon. *Atherosclerosis*. 2001;154:237–238.
23. Eroglu S, Sade LE, Yildirir A, Bal U, Ozbicer S, Ozgul AS, Bozbas H, Aydinalp A, Muderrisoglu H. Epicardial adipose tissue thickness by echocardiography is a marker for the presence and severity of coronary artery disease. *Nutr Metab Cardiovasc Dis*. 2009;19:211–217. doi: 10.1016/j.numecd.2008.05.002.

24. Iacobellis G, Ribaudo MC, Zappaterreno A, Iannucci CV, Leonetti F. Relation between epicardial adipose tissue and left ventricular mass. *Am J Cardiol*. 2004;94:1084–1087. doi: 10.1016/j.amjcard.2004.06.075.
25. Fontes-Carvalho R, Fontes-Oliveira M, Sampaio F, Mancio J, Bettencourt N, Teixeira M, Rocha Gonçalves F, Gama V, Leite-Moreira A. Influence of epicardial and visceral fat on left ventricular diastolic and systolic functions in patients after myocardial infarction. *Am J Cardiol*. 2014;114:1663–1669. doi: 10.1016/j.amjcard.2014.08.037.
26. Parisi V, Rengo G, Pagano G, D'Esposito V, Passaretti F, Caruso A, Grimaldi MG, Lonobile T, Baldascino F, De Bellis A, Formisano P, Ferrara N, Leosco D. Epicardial adipose tissue has an increased thickness and is a source of inflammatory mediators in patients with calcific aortic stenosis. *Int J Cardiol*. 2015;186:167–169. doi: 10.1016/j.ijcard.2015.03.201.
27. Iacobellis G, Willens HJ. Echocardiographic epicardial fat: a review of research and clinical applications. *J Am Soc Echocardiogr*. 2009;22:1311–1319; quiz 1417. doi: 10.1016/j.echo.2009.10.013.
28. Flotats A, Carrió I, Agostini D, Le Guludec D, Marcassa C, Schäfers M, Schaffers M, Somsen GA, Unlu M, Verberne HJ; EANM Cardiovascular Committee; European Council of Nuclear Cardiology. Proposal for standardization of 123I-metaiodobenzylguanidine (MIBG) cardiac sympathetic imaging by the EANM Cardiovascular Committee and the European Council of Nuclear Cardiology. *Eur J Nucl Med Mol Imaging*. 2010;37:1802–1812. doi: 10.1007/s00259-010-1491-4.
29. Pellegrino T, Petretta M, De Luca S, Paolillo S, Boemio A, Carotenuto R, Petretta MP, di Nuzzo C, Perrone-Filardi P, Cuocolo A. Observer reproducibility of results from a low-dose 123I-metaiodobenzylguanidine cardiac imaging protocol in patients with heart failure. *Eur J Nucl Med Mol Imaging*. 2013;40:1549–1557. doi: 10.1007/s00259-013-2461-4.
30. Cerqueira MD, Weissman NJ, Dilsizian V, Jacobs AK, Kaul S, Laskey WK, Pennell DJ, Rumberger JA, Ryan T, Verani MS; American Heart Association Writing Group on Myocardial Segmentation and Registration for Cardiac Imaging. Standardized myocardial segmentation and nomenclature for tomographic imaging of the heart. A statement for healthcare professionals from the Cardiac Imaging Committee of the Council on Clinical Cardiology of the American Heart Association. *Circulation*. 2002;105:539–542.
31. Balcioğlu AS, Çiçek D, Akinci S, Eldem HO, Bal UA, Okyay K, Müderrisoğlu H. Arrhythmogenic evidence for epicardial adipose tissue: heart rate variability and turbulence are influenced by epicardial fat thickness. *Pacing Clin Electrophysiol*. 2015;38:99–106. doi: 10.1111/pace.12512.
32. Zhou Q, Zhang L, Wang K, Xu X, Ji M, Zhang F, Wang H, Hou Y. Effect of interconnection between cervical vagus trunk, epicardial fat pad on sinus node function, and atrial fibrillation. *Pacing Clin Electrophysiol*. 2014;37:356–363. doi: 10.1111/pace.12265.
33. Lin YK, Chen YC, Chen JH, Chen SA, Chen YJ. Adipocytes modulate the electrophysiology of atrial myocytes: implications in obesity-induced atrial fibrillation. *Basic Res Cardiol*. 2012;107:293. doi: 10.1007/s00395-012-0293-1.
34. Chen PS, Turker I. Epicardial adipose tissue and neural mechanisms of atrial fibrillation. *Circ Arrhythm Electrophysiol*. 2012;5:618–620. doi: 10.1161/CIRCEP.112.974956.
35. Ardell JL. The cardiac neuronal hierarchy and susceptibility to arrhythmias. *Heart Rhythm*. 2011;8:590–591. doi: 10.1016/j.hrthm.2010.12.019.
36. Jiang YH, Jiang P, Yang JL, Ma DF, Lin HQ, Su WG, Wang Z, Li X. Cardiac dysregulation and myocardial injury in a 6-hydroxydopamine-induced rat model of sympathetic denervation. *PLoS One*. 2015;10:e0133971. doi: 10.1371/journal.pone.0133971.
37. White IA, Gordon J, Balkan W, Hare JM. Sympathetic reinnervation is required for mammalian cardiac regeneration. *Circ Res*. 2015;117:990–994. doi: 10.1161/CIRCRESAHA.115.307465.
38. Corradi D, Maestri R, Callegari S, Pastori P, Goldoni M, Luong TV, Bordi C. The ventricular epicardial fat is related to the myocardial mass in normal, ischemic and hypertrophic hearts. *Cardiovasc Pathol*. 2004;13:313–316. doi: 10.1016/j.carpath.2004.08.005.
39. Kuwahara T, Hamada M, Hiwada K. Direct evidence of impaired cardiac sympathetic innervation in essential hypertensive patients with left ventricular hypertrophy. *J Nucl Med*. 1998;39:1486–1491.
40. Slavin BG, Ballard KW. Morphological studies on the adrenergic innervation of white adipose tissue. *Anat Rec*. 1978;191:377–389. doi: 10.1002/ar.1091910310.
41. Bartness TJ, Bamshad M. Innervation of mammalian white adipose tissue: implications for the regulation of total body fat. *Am J Physiol*. 1998;275:R1399–R1411.
42. Bartness TJ, Song CK. Sympathetic and sensory innervation of white adipose tissue. *J Lipid Res*. 2007;48:1655–1672.
43. Berlan M, Lafontan M. The alpha 2-adrenergic receptor of human fat cells: comparative study of alpha 2-adrenergic radioligand binding and biological response. *J Physiol (Paris)*. 1982;78:279–287.
44. Lafontan M, Berlan M. Fat cell alpha 2-adrenoceptors: the regulation of fat cell function and lipolysis. *Endocr Rev*. 1995;16:716–738. doi: 10.1210/edrv-16-6-716.
45. Lafontan M, Langin D. Lipolysis and lipid mobilization in human adipose tissue. *Prog Lipid Res*. 2009;48:275–297. doi: 10.1016/j.plipres.2009.05.001.
46. Giordano A, Frontini A, Murano I, Tonello C, Marino MA, Carruba MO, Nisoli E, Cinti S. Regional-dependent increase of sympathetic innervation in rat white adipose tissue during prolonged fasting. *J Histochem Cytochem*. 2005;53:679–687. doi: 10.1369/jhc.4A6566.2005.
47. Bowers RR, Festuccia WT, Song CK, Shi H, Migliorini RH, Bartness TJ. Sympathetic innervation of white adipose tissue and its regulation of fat cell number. *Am J Physiol Regul Integr Comp Physiol*. 2004;286:R1167–R1175. doi: 10.1152/ajpregu.00558.2003.
48. Zhu XH, He QL, Lin ZH. Effects of catecholamines on human preadipocyte proliferation and differentiation. *Zhonghua Zheng Xing Wai Ke Za Zhi*. 2003;19:282–284.
49. Kvetnansky R, Sabban EL, Palkovits M. Catecholaminergic systems in stress: structural and molecular genetic approaches. *Physiol Rev*. 2009;89:535–606. doi: 10.1152/physrev.00042.2006.
50. Iacobellis G, Willens HJ, Barbaro G, Sharma AM. Threshold values of high-risk echocardiographic epicardial fat thickness. *Obesity (Silver Spring)*. 2008;16:887–892. doi: 10.1038/oby.2008.6.

Novelty and Significance

What Is Known?

- Epicardial adipose tissue (EAT) has a close relationship with myocardial autonomic function, directly modulates cardiac electrophysiological properties, and may promote arrhythmogenesis in pathological conditions.

What New Information Does This Article Contribute?

- In patients with heart failure (HF), EAT represents a relevant source of catecholamines, which could contribute to anatomic and functional sympathetic denervation of the failing myocardium.

EAT represents the visceral fat depot of the heart and influences myocardial homeostasis through vasocrine and paracrine mechanisms. EAT contains abundant adrenergic nerves that interact with the extrinsic nervous system to modulate the cardiac autonomic system. This study explores for the first time the relationship between EAT and cardiac sympathetic denervation in patients with HF. In 110 patients with systolic HF, we observed a significant correlation between increased echocardiographic EAT thickness and cardiac sympathetic denervation assessed by ^{123}I-metaiodobenzylguanidine myocardial scintigraphy. Furthermore, we found increased levels of catecholamines and catecholamine biosynthetic enzymes within EAT. This represents the first demonstration of a sympathetic nervous system hyperactivity in the cardiac visceral fat of HF patients. Because of the proximity to the myocardium and the high catecholamine content, EAT could induce a negative feedback on cardiac sympathetic nerves, therefore contributing to functional and anatomic denervation of the failing heart. This is particularly relevant given the importance of cardiac sympathetic denervation on cardiac homeostasis and repair. Our results pave the way for future evaluation on the potential use of EAT thickness as an index of cardiac adrenergic nerve activity and prognosis in HF patients.

Circulation Research
JOURNAL OF THE AMERICAN HEART ASSOCIATION

Increased Epicardial Adipose Tissue Volume Correlates With Cardiac Sympathetic Denervation in Patients With Heart Failure

Valentina Parisi, Giuseppe Rengo, Pasquale Perrone-Filardi, Gennaro Pagano, Grazia Daniela Femminella, Stefania Paolillo, Laura Petraglia, Giuseppina Gambino, Aurelio Caruso, Maria Gabriella Grimaldi, Francesco Baldascino, Maria Nolano, Andrea Elia, Alessandro Cannavo, Antonio De Bellis, Enrico Coscioni, Teresa Pellegrino, Alberto Cuocolo, Nicola Ferrara and Dario Leosco

Circ Res. 2016;118:1244-1253; originally published online February 29, 2016;
doi: 10.1161/CIRCRESAHA.115.307765
Circulation Research is published by the American Heart Association, 7272 Greenville Avenue, Dallas, TX 75231

Print ISSN: 0009-7330. Online ISSN: 1524-4571

SUPPLEMENTAL MATERIALS

Online Table I. Correlation between echocardiographic EAT thickness, and cardiac ^{123}I-MIBG planar and SPECT data, and LVEF.

	EAT	
	Pearson	**p value**
^{123}I-MIBG planar and SPECT data		
Early H/M	-0.305	.001
Late H/M	-0.332	.0001
Wash-out rate	.121	.210
SPECT TDS	0.701	.0001
LVEF	-.122	.272

EAT, epicardial adipose tissue; ^{123}I-MIBG, iodine-123 meta-iodobenzylguanidine; H/M, heart to mediastinum ratio; TDS, total defect score; LVEF, left ventricular ejection fraction.

Online Table II. Correlation between LVEF and cardiac ^{123}I-MIBG planar and SPECT data.

	LVEF	
	Pearson	**p value**
^{123}I-MIBG planar and SPECT data		
Early H/M	0.179	.106
Late H/M	0.388	<.0001
Wash-out rate	-0.146	.187
SPECT TDS	-0.263	.051

LVEF, left ventricular ejection fraction; ^{123}I-MIBG, iodine-123 meta-iodobenzylguanidine; H/M, heart to mediastinum ratio; TDS, total defect score.

Online Table III. Heart rate variability data on cardiac parasympathetic activity in HF patients

pNN50, %	13.05±17.23
rMMSD, msec	40.08±27.40
HF, $msec^2$	218.96±272.48

pNN50, percentage of successive normal sinus RR intervals >50 ms; rMSSD, root-mean-square of the successive normal sinus RR interval difference; HF, high frequency oscillation

Online Table IV. Correlation between EAT and cardiac parasympathetic activity assessed by HRV

	EAT	
	Pearson	**p value**
HRV parameters		
pNN50	0.102	.678
rMMSD	0.079	.747
HF	0.051	.083

EAT, epicardial adipose tissue; HRV, heart rate variability; pNN50, percentage of successive normal sinus RR intervals >50 ms; rMSSD, root-mean-square of the successive normal sinus RR interval difference; HF, high frequency oscillation

Online Figure 1